



## Design and testing of an isolated commercial EDR plant driven by solar photovoltaic energy

Baltasar Peñate<sup>a,\*</sup>, Fernando Círez<sup>b</sup>, Francisco J. Domínguez<sup>a</sup>, Vicente J. Subiela<sup>a</sup>, Luisa Vera<sup>a</sup>

<sup>a</sup>Water Department, Research and Technological Development Division, Canary Islands Institute of Technology (ITC), Playa de Pozo Izquierdo, s/n. 35119 Santa Lucía, Gran Canaria, Spain

Tel. +34 928 72 75 03; Fax +34 928 72 75 90; email: baltasarp@itccanarias.org

<sup>b</sup>Natural Resources Area, CIRCE Foundation, University of Zaragoza, C/Mariano Esquillor Gómez, 15, 50.018 Zaragoza, Spain

Received 15 March 2012; Accepted 18 July 2012

---

### ABSTRACT

The production of potable water from brackish water, tertiary treatments of treated wastewaters for irrigation and other allowed uses, and several industrial processes which use recycled water are the most important applications of electro dialysis (ED). During the last years, the number of pilot initiatives focused on renewable energy powered desalination has grown, being one of the most promising combinations of the ED powered by photovoltaic (PV) systems. ED combined with renewable energies becomes attractive for being a mature technology, which requires direct current (DC) power and is easily adapted for variable energy conditions. The present paper shows the design, installation, testing, and monitoring of a 100% isolated PV–ED system which is feasible for a commercial scale. The testing tasks have been performed in a 4 m<sup>3</sup>/h commercial-one stack electro dialysis reversal plant powered by two solar PV fields in parallel. For the DC energy required in the stack, a solar PV field has been designed and tested. It permits modulation by different solar panels connections, and thus makes possible to maintain the output current according to the real solar radiation and different raw water salinity.

*Keywords:* Desalination; Renewable energy; Commercial-scale EDR plant; Solar PV; Off-grid

---

### 1. Introduction

Fresh-water and reclaimed water are more and more required resources in industrialized countries. The increment of population, services, irrigation, environmental risks, and climate change is reducing the water availability per person. This matter is particularly critical in developing countries. In regions where the scarcity of

water resources goes in parallel with the availability of renewable energy, a common strategy is to enlist local energy resources in order to provide water [1].

The production of potable water from brackish waters, the tertiary treatments of wastewaters for irrigation and other allowed uses, and several industrial processes which use recycled water are the most important applications of electro dialysis (ED) [2–4]. In general, ED is an electrochemical separation process that utilizes a direct current (DC) electric field to remove the

---

\*Corresponding author.

salt ions in the saline water. This saline solution is forced to pass between several pairs of ions selective membranes (cation and anion membrane cell pairs). Ions are removed from the brackish water through the membranes; as opposed to other membrane processes where the water passes through the membrane. A modern concept of this technology for industrial purposes is called electro dialysis reversal (EDR). In this case, the polarity of the DC field (anode and cathode) is inverted from twice to four times per hour for preventing scaling. During this polarity inversion, the product and concentrate channels are exchanged.

ED combined with renewable energies becomes attractive for being a mature technology, which requires DC power and being easily adaptable for variable energy conditions. The technology shows good flexibility and smoothly adaptation not only with wind energy [5], but also with solar photovoltaic (PV) [6–8]. In both cases, a similar behavior of the plant is detected when it has been connected to the electrical grid.

Most of the off-grid pilot ED experiences tested have been done with solar PV [9,10]. PV energy provides two great advantages in terms of being connected to ED. The first one is the possibility to directly power the ED stack. In addition, the excess of energy can be stored in batteries to be used as an energy back-up system or can be converted into AC by means of inverters to power the pumping and control devices. The second one is its modularity and the possibility of connecting more or less PV modules to increase the water quality or to counter a decrease in solar irradiation. One of the consequences of connecting an ED plant to a batteryless system is that the water production and quality varies with the solar radiation. An advantage of this solution is related to reduction of environmental topic and increase the sustainability of the process [8].

The objective of the present work is to disseminate the preliminary results of the design and testing of an isolated  $4\text{ m}^3/\text{h}$  commercial EDR plant driven by solar PV energy, installed in the Instituto Tecnológico de Canarias–ITC facilities in Pozo Izquierdo–Gran Canaria island (Spain) [11]. Two PV fields support the total energy required for the EDR unit. The first one produces DC electric energy, which is used directly in the stack without batteries. The second one consists of batteries, regulator, and inverter for producing AC electric energy used in water pumping, valves, and 24/365 control.

## 2. EDR-PV system description

### 2.1. EDR unit

The EDR unit presented in this paper was designed to treat brackish water driven by wind energy within seawater desalination with an autonomous wind energy system (SDAWES) project, co-financed by the JOULE III Program of the European Union [12]. This initiative tested a wind-powered desalination prototype in the facilities of ITC in Pozo Izquierdo (Gran Canaria Island). This EDR plant (Aquamite V-II, Ionics) had two membrane stacks (four hydraulic stages and two electrical stages per stack) and a nominal capacity of  $2 \times 96\text{ m}^3/\text{d}$ .

For this new experience with solar PV integration, some hydraulic modifications have been done to work with one stack ( $4\text{ m}^3/\text{h}$  nominal capacity). Fig. 1 shows the modified EDR plant flow diagram and Figs. 2 and 3 show views of the plant.

The product flow rate and the pressure required for operation are controlled by means of the feed pump; a recycled concentrate flow is moved from the

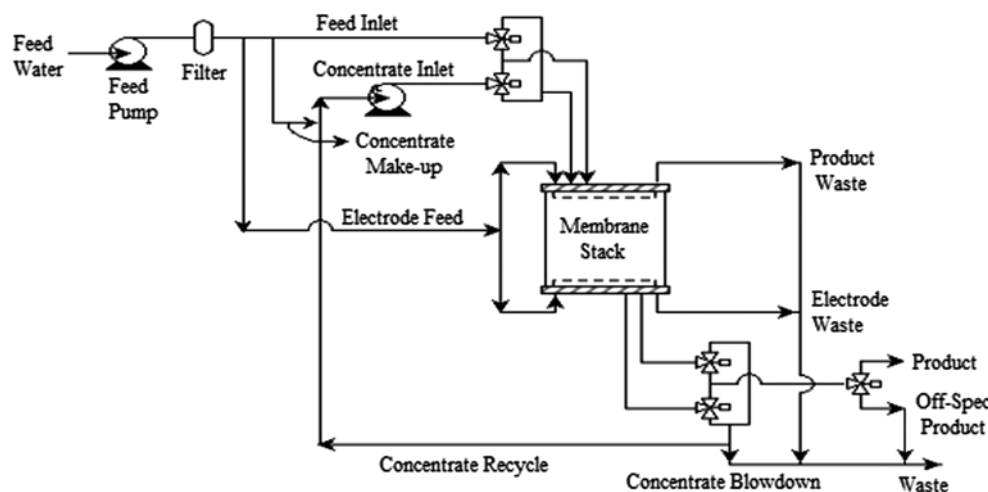


Fig. 1.  $4\text{ m}^3/\text{h}$  EDR plant flow diagram.



Fig. 2. EDR plant general view.



Fig. 3. EDR stack during maintenance tasks.

stack with a brine pump. The pumps are controlled by variable frequency drivers which change pumps speed to control feed pressure and the stack inlet differential pressure, respectively.

The EDR unit is powered and controlled through electrical and control systems. The plant is controlled by its own programmable logic controller (PLC) controller, which is responsible for the operating mode with PV (DC/AC) and transferring the operation data to a data acquisition system.

The stack used is the initial installed within SDAWES project (1999). The EDR plant used special

spacers (third generation) to provide high efficiency to the stack. Additional information on the specifications of the EDR unit is given in Table 1.

## 2.2. Solar PV systems

The solar PV system is composed of two different solar fields, which produce the total energy required for the EDR unit. The energy produced by a 5.8 kW peak power PV field is used in feed and concentrated pumps, valves and 24/365 control, and a direct

Table 1  
EDR plant technical specifications

| Technical specifications       | Parameters            |
|--------------------------------|-----------------------|
| <i>EDR plant</i>               |                       |
| Input power                    | 380 V, 3-phase, 50 Hz |
| Full load current              | 140 A                 |
| Feed pump power                | 4 kW                  |
| Brine pump power               | 3 kW                  |
| Max. Feed flow (1 stack)       | 122 m <sup>3</sup> /d |
| Nominal product flow (1 stack) | 4 m <sup>3</sup> /h   |
| Min. product flow (1 stack)    | 3 m <sup>3</sup> /h   |
| <i>EDR stack</i>               |                       |
| Hydraulic stages               | 4                     |
| Electrical stages              | 2                     |
| Stage 1                        | 132 Vdc, 46 A max.    |
| Stage 2                        | 91 Vdc, 16 A max.     |
| No. of cell pairs              | 340                   |
| Cell pairs configuration       | 95/75//95/75          |
| No. of anionic membranes       | 340                   |
| No. of cationic membranes      | 336                   |
| No. of spacers (Mark IV)       | 680                   |

connection batteryless PV field is used for producing the DC electric energy which is used directly in the EDR stack.

The first PV field was designed under conventional off-grid criteria and consists of PV panels with solar tracking systems (for other research topics in parallel), a battery bank, and charger/inverter device



Fig. 4. Solar PV field for AC electric energy.

for producing AC electric energy. Fig. 4 shows a view of the field and Fig. 5 shows a picture of the batteries. Three solar tracker generators in parallel—28 modules HIS-M206SF/206 W supplies energy to the off-grid AC/DC electric network—composed by a 800 Ah (C10) battery bank (FIAMM-OPzS stationary lead-acid battery vessels) for 7 h of autonomy and a charger/inverter equipment with a nominal power of 9 kW. The electronic devices make possible that the PV field



Fig. 5. Battery bank.



works at the maximum power point [8], and it allows modulating the output AC signal required in the EDR plant (3phases-400 VAC).

This electricity is used to power the PLC, to drive the EDR unit to provide water circulation and chemical dosing and also to drive the motor-operated valves.

The DC electric energy supply for EDR stack was designed under variable conditions without batteries and regulation. The PV field produces energy that is used directly in the two electrical stages of the stack. According to that, the PV field is modular and actually consists of two PV fields. The design criteria and modular configuration of both depend on the voltage drop, due to the stack (concentrations and membranes) resistance, and the current required by each electrical stage. The total energy required per electrical stage for the transfer of ions from feed to the concentrate channel is given by the total voltage drop encountered between the electrodes multiplied by the current passing through the stack. So that, for a given brackish water concentration and target product salinity, the required DC electric energy is directly proportional to the current density [2].

The size of the variable PV fields (kWp) and the instantaneous control of required DC energy are under patent registration study.

For this experimentation, the first electrical stage is connected with a 2.45 kWp PV field (12 PV panels/HIS-M206SF/206 W—35° inclination) and the second one is connected with a 1.24 kWp PV field (6 panels/HIS-M206SF/206 W—35° inclination) at the maximum power point (see Fig. 6 and Table 2). These fields are designed with the aim of changing instantaneously

Table 2  
Solar PV field maximum power values ( $G = 1,000 \text{ W/m}^2$ )

| Technical specifications                  | Parameters |
|---|------------|
| <i>Solar PV 1—Electrical stage 1 (DC)</i> |            |
| Voltage (V)                               | 110        |
| Current (A)                               | 22.52      |
| <i>Solar PV 2—Electrical stage 2 (DC)</i> |            |
| Voltage (V)                               | 83         |
| Current (A)                               | 22.38      |

their PV panel configuration, i.e. PV field modulation (PVFM) according to the solar irradiation for working in maximum power point and obtaining the best product salinity in any case.

It has been designed and configured five possible PVFMs (1, 2, ..., 5). Each of them is able to work at different  $I_{DC}$ -V values depending on the serial-parallel PV arrangement. For a wide range of solar irradiation ( $G = 250$ – $1,100 \text{ W/m}^2$ ), the PV field is able to operate with the EDR plant obtaining a desired and good product quality depending of the PVFM used in each instant.

### 2.3. Integration and Control system

Both EDR plant and PV fields are controlled using electrical devices and the PLC controller. Different electrical boxes for controlling the AC/DC energy produced have been installed. The PLC is responsible of the operation of the EDR plant (pumps, valves, and stack) and the selection of the adequate PVFM (one option among five possible ones). Besides, the data



Fig. 6. Solar PV field for DC electric energy.

are registered in a datalogger multifunction. In fact, the PLC has been programmed according to the logic design of deciding in an automatic way or under manual instructions of changing the PVFM according to the  $G$  value for working in the point of maximum power and obtaining the best product salinity in any case.

### 3. Results and discussion

Once the wind-EDR [4] system was modified in order to operate the EDR plant driven by off-grid PV fields, an indepth testing process was carried out. The main aim of this experimentation was to obtain the effect of  $G$ , feed water quality and PVFMs behavior over the fresh water produced (quality and quantity).

All the tests were carried out using different artificial brackish water concentrations (from 3,500 to 5,300  $\mu\text{S}/\text{cm}$  feedwater conductivity) and the plant was tested with variable and constant (600 and 800  $\text{W}/\text{m}^2$ ) solar irradiation. For these tests, the raw water and brine recirculating flows were constant and equal to 6,000 and 2,000 l/h, respectively. The AC energy consumption was 3,260 Wh (63/37% for feeding/recirculating pumping); energy supplied by AC/DC PV field is described previously.

#### 3.1. Influence of the solar irradiation ( $G$ ) over the designed PVFMs

In order to observe the influence that  $G$  and the defined PVFMs have over the product quality and the operation of the EDR stack, similar tests in consecutive days were carried out. These tests consisted of operating the EDR plant among the whole day with different PVFMs with a 5,300  $\mu\text{S}/\text{cm}$  feedwater solution. By this, for each modulation and  $G$  the operating

variable data and the product quality (conductivity) were registered. Thanks to these registers, it has been possible to obtain for each solar irradiation, the PVFM that allows obtaining a product with a desired conductivity.

In Figs. 7 and 8, it can be seen the evolution of the product conductivity and the DC current across the electrical stages of the EDR stack for a time between polarity changes ( $t_{\text{bpc}} = 15$  min). The transitory information (data allocated between the change of polarity and until the product off specification [offspec] conductivity is reached) has been omitted. This time of offspec is the period until the product conductivity is under a set value that can be assumed as correct; (1,500  $\mu\text{S}/\text{cm}$  in this case).

The dispersion that Fig. 7 shows is due to the transitory effects that take place inside the EDR stack until the stationary state is reached. Once the stationary state is reached after each polarization change, it is possible to obtain desired product conductivities for each irradiation value by means of choosing one PVFM or another one.

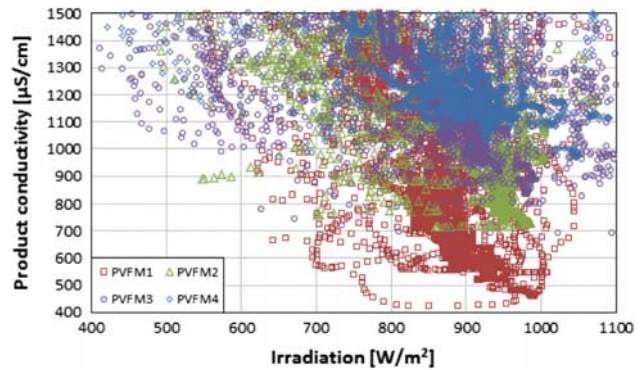


Fig. 7. PVFM and  $G$  ( $\text{W}/\text{m}^2$ ) vs. product conductivity (feed water conductivity = 5,300  $\mu\text{S}/\text{cm}$ ).

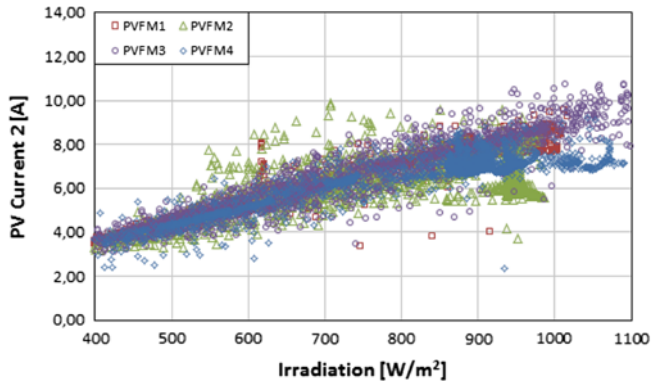
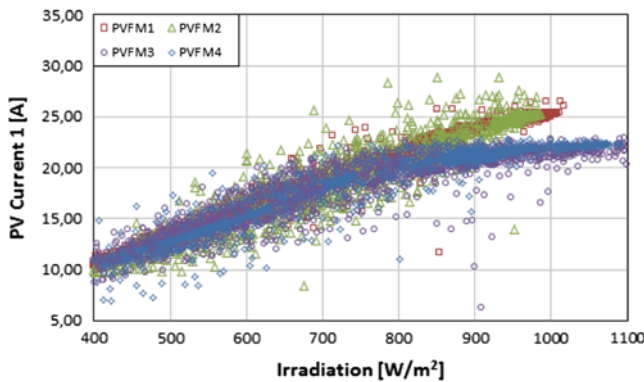


Fig. 8. PVFM and  $G$  [ $\text{W}/\text{m}^2$ ] over the DC current across the EDR stack (feed water conductivity = 5,300  $\mu\text{S}/\text{cm}$ ; Current 1: Solar PV field—Electrical stage 1; Current 2: Solar PV field—Electrical stage 2).

Fig. 8 shows a linear and direct relation between  $G$  and the  $I_{DC}$  across the both EDR electrical stage. It is also possible to see that PVFM1 and PVFM2 configurations allow obtaining higher values of current at the electrical stage 1 of the stack. There are no important differences in the second electric stage between the possible PVFMs.

### 3.2. Influence of the feed water quality

In order to determinate the influence that the conductivity of the feedwater has over the electrical operating data and the quality of the product water, similar tests (Seen Fig. 7), were carried out for a  $3,500 \mu\text{S}/\text{cm}$  feeding solution. The results, once the stationary state (after the polarity change) is reached, are shown in Tables 3 and 4.

As it can be seen in Tables 3 and 4, it is possible to obtain certain product conductivity depending on the raw water conductivity, the solar irradiation, and the PVFM. As a preliminary conclusion, the proposed PVFM are able to desalt solutions which conductivity is lower than  $5,000 \mu\text{S}/\text{cm}$  for irradiation higher than  $600 \text{W}/\text{m}^2$  and that EDR operation can quickly adapt to the available irradiation.

The influence of these variables ( $G$  and PV configurations) for fixed feedwater conductivity can be seen at Fig. 9.

### 3.3. Effect of the polarity change over the DC PV field

An important issue, not very studied at EDR field, is the effect that the time assigned for the polarity

Table 3  
Influence of the feed water conductivity ( $\mu\text{S}/\text{cm}$ ) at high irradiation  $G$  range ( $\text{W}/\text{m}^2$ )

| Feed conductivity ( $\mu\text{S}/\text{cm}$ ) | $G$ ( $\text{W}/\text{m}^2$ ) | PVFM No. | $I_{DC1}$ (A) | $I_{DC2}$ (A) | DC Power (kW) | Product conductivity ( $\mu\text{S}/\text{cm}$ ) |
|---|-------------------------------|----------|---------------|---------------|---------------|--|
| 3,580   | 800                           | 1        | 17.8          | 3.8           | 2.11          | 114  |
| 3,431   | 800                           | 2        | 17.9          | 2.7           | 1.98          | 229  |
| 3,508   | 798                           | 3        | 15.5          | 5.2           | 1.67          | 169  |
| 3,466   | 798                           | 4        | 15.5          | 4.1           | 1.47          | 401  |
| 3,421   | 803                           | 5        | 11.2          | 5.9           | 0.94          | 740  |
| 5,364   | 800                           | 1        | 20.7          | 6.9           | 1.97          | 1,165  |
| 5,331   | 801                           | 2        | 22.9          | 7.0           | 2.11          | 1,186  |
| 5,078   | 792                           | 3        | 19.1          | 7.1           | 1.75          | 1,360  |
| 5,337   | 797                           | 4        | 20.4          | 6.7           | 1.76          | 1,390  |
| 5,299   | 800                           | 5        | 13.4          | 6.1           | 0.94          | 1,831  |

Notes: The DC current is presented in absolute value; Both DC current and product conductivity values presented are the most representatives along several polarities.

Table 4  
Influence of the feed water conductivity ( $\mu\text{S}/\text{cm}$ ) at medium irradiation range ( $\text{W}/\text{m}^2$ )

| Feed conductivity ( $\mu\text{S}/\text{cm}$ ) | $G$ ( $\text{W}/\text{m}^2$ ) | PVFM No. | $I_1$ (A) | $I_2$ (A) | DC Power (kW) | Product conductivity ( $\mu\text{S}/\text{cm}$ ) |
|---|-------------------------------|----------|-----------|-----------|---------------|--|
| 3,582   | 581                           | 1        | 15.3      | 5.3       | 1.49          | 297  |
| 3,500   | 611                           | 2        | 16.0      | 3.2       | 1.64          | 314  |
| 3,581   | 587                           | 3        | 14.9      | 5.4       | 1.42          | 351  |
| 3,400   | 600                           | 4        | 14.4      | 4.2       | 1.32          | 484  |
| 3,558   | 607                           | 5        | 11.5      | 5.5       | 0.89          | 851  |
| 5,298   | 600                           | 1        | 15.8      | 5.3       | 1.03          | 2,239  |
| 5,291   | 611                           | 2        | 15.7      | 5.3       | 1.04          | 2,360  |
| 5,292   | 600                           | 3        | 15.2      | 5.2       | 0.98          | 2,365  |
| 5,289   | 598                           | 4        | 15.0      | 5.1       | 0.94          | 2,413  |
| 5,279   | 611                           | 5        | 13.6      | 5.1       | 0.86          | 2,411  |

Notes: The DC currents are in absolute values; Both DC currents and product conductivity values presented are the most representatives along several polarities.

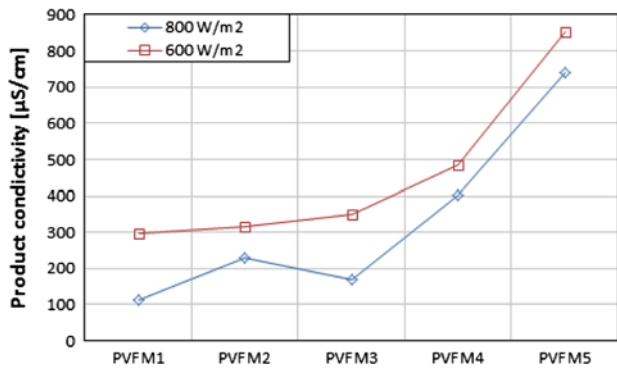


Fig. 9. Influence of PVFM and G [W/m<sup>2</sup>] over product conductivity (feed water conductivity = 3,500 µS/cm).

change has over the EDR overall resistance stack, the electric consumptions, or the offspec time. Alternating the polarity means maintenance of pH stability in all cell compartments and therefore effective confrontation of the undesirable phenomena of scaling [13].

Table 5

Influence of the time between polarity changes over offspec time (feed water conductivity = 3,500 µS/cm)

| Irradiation (W/m <sup>2</sup> ) | Polarity (+/-) | t <sub>bpc</sub> (min) | t <sub>osp</sub> (s) | Max. I <sub>DC</sub> PV1 (A) | Max I <sub>DC</sub> PV2 (A) |
|---------------------------------|----------------|------------------------|----------------------|------------------------------|-----------------------------|
| 835                             | +              | 6                      | 33                   | -21.2                        | -7.9                        |
| 835                             | -              | 6                      | 33                   | 21.3                         | 7.8                         |
| 834                             | +              | 8                      | 33                   | -21.1                        | -7.8                        |
| 826                             | -              | 8                      | 34                   | 21.4                         | 7.9                         |
| 825                             | +              | 12                     | 34                   | -21.3                        | -7.9                        |
| 836                             | -              | 12                     | 34                   | 21.4                         | 7.8                         |
| 835                             | +              | 15                     | 33                   | -21.4                        | -7.9                        |
| 840                             | -              | 15                     | 35                   | 21.6                         | 7.9                         |
| 821                             | +              | 18                     | 35                   | -21.5                        | -7.9                        |
| 806                             | -              | 18                     | 37                   | 21.8                         | 8.0                         |

Usually, the time between two consecutive polarity changes is from 15 to 30 min [14].

The Table 5 shows the offspec time, t<sub>osc</sub>, when a 3,500 µS/cm feed solution is used, working at constant G (805–840 W/m<sup>2</sup>) and PVFM2 array configuration. In addition, Table 5 also shows the maximum I<sub>DC</sub> reached when the polarity changes.

One of the main conclusions obtained from these tests is the influence that the increase of the t<sub>bpc</sub> has over the t<sub>osp</sub>. It can be seen that the higher time between polarity changes, the higher offspec time is obtained. However, an increase in the offspec time is not significant (only 4s when the t<sub>bpc</sub> is increased from 6 to 18 min). This leads to think that it is better a higher t<sub>bpc</sub> in order to have a higher production on specifications (i.e when t<sub>bpc</sub> is set at 6 min, there are 297s of offspec flow in an hour; but when 18 min is set, there are just 105s of offspec flow).

The lower limit for t<sub>bpc</sub> has been set at six minutes due to the fact that until this time, the EDR plant is not stabilized as can be seen in Fig. 10.

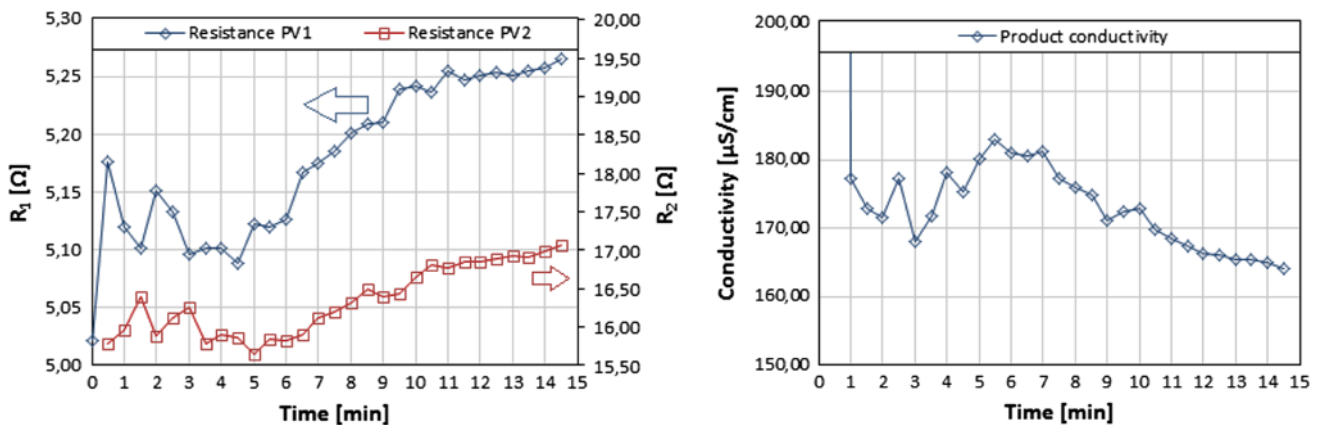


Fig. 10. Overall stack resistance and product conductivity timing evolution (feed water conductivity = 3,500 µS/cm; R: resistance of the stack electrical stage).



Two aspects should be remarked in the Fig. 10. The first one is that, in opposition to the ED batch, in an EDR the resistance increase is not very significant during the desalination test with an increment of 5% for the electrical stage 1 and 7.9% for the second electrical stage. During an ED batch test with the same initial conductivity feed solution increments on the overall stack resistance of 150% can appear [15]. The second one aspect to remark is that it can be seen in Fig. 10, until the 6th min. is reached the stack resistance is fluctuating. The same behavior can be seen at product flow conductivity.

When the influence over the maximum  $I_{DC}$  at electrical stages after the polarity change is analyzed, it can be seen that the higher  $t_{bpc}$  the higher maximum current is obtained. This is a point to take into account, because the possible effects on the EDR stack in case of these currents were higher than the limiting current of the membranes.

### 3.4. Off-grid automatic mode operation

Fig. 11 represents a period of operation in automatic mode. In this mode, the PLC is able to choose the PVFM that produces the lowest possible product conductivity. The information corresponds to 5 h operation with a  $5,300 \mu\text{S}/\text{cm}$  feedwater conductivity and a  $t_{bpc}$  of 15 min during a good solar radiation day.

In Table 6, it can be seen a summary of operation parameters for the data shown in Fig. 11.

In Fig. 12, it can be seen a typical power distribution during the plant operation. When the  $G$  value is

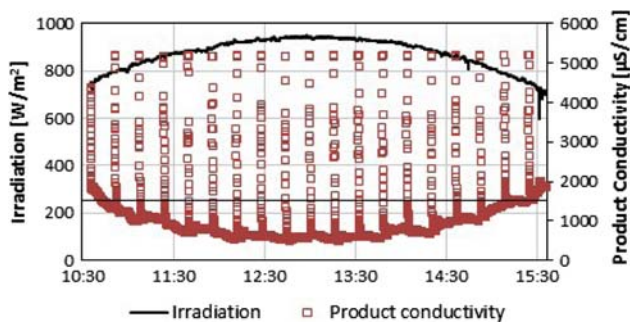


Fig. 11. EDR-FV automatic mode operation for  $5,300 \mu\text{S}/\text{cm}$  feed water.

Table 6  
EDR-FV operating results in automatic mode for a  $5,300 \mu\text{S}/\text{cm}$  feed water

| Feed water (L) | Product water (L) | Average conductivity product water ( $\mu\text{S}/\text{cm}$ ) | Off-spec water (L) | Average SEC (kWh/m) | Energy consumption (kWh) |
|----------------|-------------------|--|--------------------|---------------------|--------------------------|
| 30,618.8       | 16,894.6          | 1,050  | 3,418.1            | 0.79                | 17.14                    |

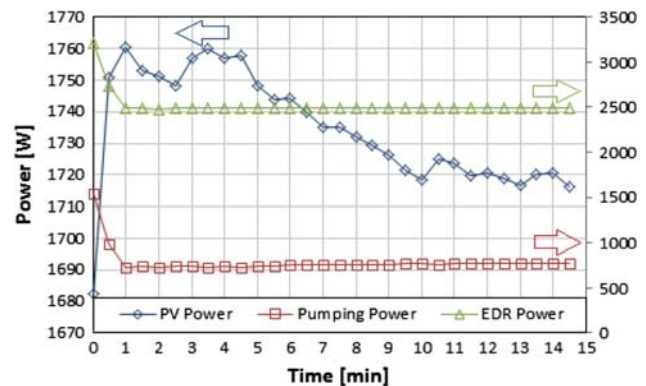


Fig. 12. Electrical power distribution during one polarity time ( $3,500 \mu\text{S}/\text{cm}$  feed water conductivity and  $G = 835 \text{ W}/\text{m}^2$ ).

high, the EDR energy consumption is mainly due to the DC stack consumption meanwhile the pumping energy could represent the 30% of the total energy consumption. In numerical terms, for a polarity changing time of 15 min, a  $3,500 \mu\text{S}/\text{cm}$  feed solution,  $G = 835 \text{ W}/\text{m}^2$ , PVFM2, and a product flow of  $4 \text{ m}^3/\text{h}$ , the energy consumption is  $0.148 \text{ kWh}$  ( $0.045$  pumping AC energy;  $0.103$  stack DC energy). The total water production during the 15 min is  $950 \text{ L}$  (under of off-spec conductivity of  $1,500 \mu\text{S}/\text{cm}$ ) and the average product conductivity obtained is  $185 \mu\text{S}/\text{cm}$ . Only  $60 \text{ L}$  are discharged. The specific energy consumption (SEC) of the plant in these conditions is  $0.618 \text{ kWh}/\text{m}^3$  ( $0.188 \text{ kWh}/\text{m}^3$  AC energy for pumping and control;  $0.43 \text{ kWh}/\text{m}^3$  stack DC energy).

The presented EDR-FV SEC values for  $3,500 \mu\text{S}/\text{cm}$  feedwater solution are very promising in terms of energy consumptions when are compared with brackish water reverse osmosis desalination plant for similar feed water solutions and recovery rate, i.e.  $0.613 \text{ kWh}/\text{m}^3$  (12 bar; 80% high pressure pump performance rate).

### 3.5. Feasibility of the EDR-PV coupling

In order to check the feasibility of desalting brackish water by means of the use of an isolated EDR stack driven by DC PV energy, software simulations (using WATSYS 2.1 EDR plant software by General

Table 7

EDR plant operation comparison (on-grid vs. off-grid tests) (3,500  $\mu\text{S}/\text{cm}$  feed conductivity; product flow = 4  $\text{m}^3/\text{h}$ ; off-grid  $G = 835\text{--}807 \text{ W}/\text{m}^2$ ; positive polarity results)

| Source            | Configuration | $V_1$<br>(V) | $V_2$<br>(V) | $I_1$<br>(A) | $I_2$<br>(A) | Product conductivity ( $\mu\text{S}/\text{cm}$ ) |
|-------------------|---------------|--------------|--------------|--------------|--------------|--|
| –                 | –             |              |              |              |              |  |
| <i>Softw sim.</i> | –             | 86           | 78           | 15.9         | 6.4          | 449.9  |
| On-grid           | –             | 86           | 78           | 15.0         | 6.2          | 424  |
| Off-grid          | PVFM3         | 79.3         | 82.9         | 15.9         | 5.7          | 180  |
| <i>Softw sim.</i> | –             | 85           | 64           | 15.8         | 5.3          | 606.6  |
| On-grid           | –             | 85           | 64           | 15.6         | 5.0          | 565  |
| Off-grid          | PVFM4         | 79.1         | 58.5         | 15.9         | 4.3          | 400  |
| <i>Softw sim.</i> | –             | 66           | 61           | 12.3         | 6.6          | 909.1  |
| On-grid           | –             | 60           | 55           | 12.1         | 6.4          | 887  |
| Off-grid          | PVFM5         | 55.6         | 54           | 11.5         | 6.1          | 724  |

Table 8

EDR plant operation comparison (on-grid vs. off-grid tests) (4,950  $\mu\text{S}/\text{cm}$  feed conductivity; product flow = 4  $\text{m}^3/\text{h}$ ; off-grid  $G = 878\text{--}1,024 \text{ W}/\text{m}^2$ ; positive polarity results)

| Source            | Configuration | $V_1$<br>(V) | $V_2$<br>(V) | $I_1$<br>(A) | $I_2$<br>(A) | Product conductivity ( $\mu\text{S}/\text{cm}$ ) |
|-------------------|---------------|--------------|--------------|--------------|--------------|--|
| –                 | –             |              |              |              |              |  |
| <i>Softw sim.</i> | –             | 107          | 84           | 24.7         | 9.0          | 646.1  |
| On-grid           | –             | 107          | 84           | 26.0         | 9.0          | 759  |
| Off-grid          | PVFM1         | 88.9         | 66.9         | 23.2         | 7.5          | 645  |
| <i>Softw sim.</i> | –             | 83           | 82           | 19.3         | 11.8         | 985.1  |
| On-grid           | –             | 83           | 82           | 22.0         | 11.3         | 902  |
| Off-grid          | PVFM3         | 80.9         | 70.7         | 18.1         | 10.03        | 874  |

Electric) and on-grid EDR plant operation data (using a DC/AC rectifier in each electric stage of the stack) were compared to isolated PV operation.

In these simulations, several variables are taken into account with the aim of being obtained in the same conditions of off-grid tests done, i.e. net production rate (product flow), EDR feed, electrode waste flow, make-up flow, minimum velocity inside the stack, stack inlet pressure, stack outlet pressure, % polarization an burning, temperature, and feed composition. The results of these simulations and the comparison with on-grid and off-grid experimental results are shown in Tables 7 and 8.

It can be seen how the isolated EDR plant driven by solar PV fields is not only feasible but even presents better working features than expected. In general, it is observed that both on-grid and off-grid operation present better conductivity values that simulated operation. It can be explained due to the security values that are used at WATSYS simulations. In addition, it can be seen that on-grid operation presents higher conductivity values than off-grid. The AC/DC conversion that takes place in the rectifiers (that it is necessary to convert the

grid energy to DC energy), leads to some electrical losses (efficiency lower than unity) that causes worse values in terms of maximum desalination.

#### 4. Conclusions

The production of potable water from brackish waters, tertiary treatments, and several industrial processes which use recycled water are the most important applications of ED. ED combined with renewable energies becomes attractive for being a mature technology which requires DC power for the stacks and being easily adaptable for variable energy conditions. ED driven by solar PV energy is a feasible combination, which uses not only the DC electric energy directly produced by the PV panels and it also exploits the excess of energy inverted (DC/AC) for pumping and control.

This paper shows the design and testing results of a 100% isolated PV–commercial ED plant combination. The testing tasks have been performed in a 4  $\text{m}^3/\text{h}$  commercial-one stack EDR plant with an energy supply from two different solar PV fields. The energy produced by a

conventional isolated PV field is used in feed and concentrated pumps, valves, and 24/365 control and a direct connection batteryless PV field is used for producing DC electric energy which is used directly in the stack.

The key of this combination is the design and control of the DC PV field. For this experimentation, the PV field is designed and tested with the aim of changing instantaneously their solar panel configuration according to the solar irradiation for working in the point of maximum power and obtaining the best product salinity in any case. Five possibilities are defined and controlled by a PLC, depending on the serial–parallel panel arrangement. For a wide range of solar irradiation (250–1,100 W/m<sup>2</sup>), the EDR plant is able to obtain a desired and good product quality depending on the modulation used for each instant.

First data indicates that this combination is a very promising option in terms of operation flexibility, energy performance (consumptions similar to RO for low-salinity brackish water), water quality production, and minimization of off-specification product operation time along the polarity change phases.

Moreover, the off-grid operation is not only feasible but even presents better working features than expected in comparison with simulated and on-grid connections. In general, it is observed that both on-grid and off-grid operation presents better conductivity values that simulated operation. On-grid operation presents higher conductivity values that off-grid solution. The AC/DC conversion that takes place in the rectifiers (on-grid mode) leads to some electrical losses which do not exist in the modulated DC PV field used in off-grid operation.

## Nomenclature

|           |   |
|-----------|---|
| AC        | alternating current                                       |
| DC        | direct current  |
| ED        | electrodialysis   |
| EDR       | electrodialysis reversal                                  |
| G =       | solar radiation (W/m <sup>2</sup> )                       |
| $I_{DC}$  | DC current (A)  |
| Offspec   | off of specification (product water conductivity)         |
| PV        | photovoltaic  |
| PVFM      | PV field modulation                                       |
| SEC       | specific energy consumption, (kWh/m <sup>3</sup> product) |
| $t_{bpc}$ | time between polarity changes, [min]                      |
| $t_{osp}$ | time offspec (s)  |
| V         | voltage (V)   |

## Acknowledgments

This work is framed within the R+D+i project called CENAME (ENE2009-14515-CO). The authors wish to thank the Spanish Ministry of Economy and Competitiveness for their financial project assistance. The authors greatly acknowledge the collaboration of CANARAGUA and ELMASA companies providing their experience.

## References

- [1] B. Peñate, L. García-Rodríguez, Current trends and future prospects in the design of seawater reverse osmosis desalination technology, *Desalination* 284 (2012) 1–8.
- [2] H. Strathmann, Electrodialysis, a mature technology with a multitude of new applications, *Desalination* 264 (2010) 268–288.
- [3] E. Selmane Bel Hadj Hmidaa, A. Ouejhani, G. Lalléve, J.F. Fauvarque, M. Dachraoui, A novel anionic electro dialysis membrane can be used to remove nitrate and nitrite from wastewater, *Desalin. Water Treat.* 23 (2010) 13–19.
- [4] E.T. Sajtar, D.M. Bagley, Electrodialysis reversal: Process and cost approximations for treating coal-bed methane waters, *Desalin. Water Treat.* 2 (2009) 278–286.
- [5] J. Veza, B. Peñate, F. Castellano, Electrodialysis desalination designed for off-grid wind energy, *Desalination* 160 (2004) 211–221.
- [6] N. Ishimaru, Solar photovoltaic desalination of brackish water in remote areas by electro dialysis, *Desalination* 98 (1994) 485–493.
- [7] H.M.N. Almadani, Water desalination by solar powered electro dialysis process, *Renewable Energy* 28 (2003) 1915–1924.
- [8] J.M. Ortiz, E. Expósito, F. Gallu, V. García-García, V. Montiel, A. Aldaz, Electrodialysis of brackish water powered by photovoltaic energy without batteries: direct connection behaviour, *Desalination* 208 (2007) 89–100.
- [9] L. García-Rodríguez, Renewable energy applications in desalination: State of the art, *Solar Energy* 75 (2003) 381–393.
- [10] C. Charcosset, A review of membrane processes and renewable energies for desalination, *Desalination* 245 (2009) 214–231.
- [11] V.J. Subiela, J.A. de la Fuente, G. Piernavieja, B. Peñate, Canary islands institute of technology (ITC) experiences in desalination with renewable energies (1996–2008), *Desalin. Water Treat.* 7 (2009) 220–235.
- [12] J.A. Carta, J. González, V. Subiela, The SDAWES project: An ambitious R&D prototype in wind-powered desalination, *Desalination* 161 (2004) 33–47.
- [13] K. Dermentzis, D. Papadopoulou, A. Christoforidis, A. Dermentzi, A new process for desalination and electrode ionization of water by means of electrostatic shielding zones – ionic current sinks, *J. Eng. Sci. Tech. Rev.* 2(1) (2009) 33–42.
- [14] R. Valerdi, J.A. Ibáñez, Electrodialysis [Electrodialysis]. Principios y aplicaciones [Key aspects and applications]. *Desalación de aguas. Aspectos tecnológicos, medioambientales, jurídicos y económicos*. Ed. Instituto Euromediterráneo del Agua, 2009, Spain.
- [15] Internal report of CENAME project (ENE2009-14515-CO) - ED batch plant testing (Eurodia EUR2B-10P) by the authors (CIRCE, 2011).